Water Research 220 (2022) 118619

Contents lists available at ScienceDirect

Water Research

journal homepage: www.elsevier.com/locate/watres

Lithologic controls on the mobility of Cd in mining-impacted watersheds revealed by stable Cd isotopes

Yuhui Liu [a,b], Yafei Xia [a,b], Zhengrong Wang [c], Ting Gao [a,*], Jian-Ming Zhu [d], Meng Qi [a,b], Jing Sun [a], Chengshuai Liu [a,e,*]

[a] State Key Laboratory of Environmental Geochemistry, Institute of Geochemistry, Chinese Academy of Sciences, Guiyang 550081, PR China
[b] University of Chinese Academy of Sciences, Beijing 100049, PR China
[c] Department of Earth & Atmospheric Sciences, The City College of New York, CUNY, New York 10031, USA
[d] State Key Laboratory of Geological Processes and Mineral Resources, China University of Geosciences, Beijing 100083, PR China
[e] National-Regional Joint Engineering Research Center for Soil Pollution Control and Remediation in South China, Guangdong Key Laboratory of Integrated Agro-environmental Pollution Control and Management, Guangdong Institute of Eco-environmental Science & Technology, Guangdong Academy of Sciences, Guangzhou 510650, PR China

ARTICLE INFO

Keywords:
Cd isotopes
Source tracing
Migration processes
Mining-affected watersheds
Lithology

ABSTRACT

Cd-rich wastes from open-pit mining can be transported into rivers, which are often followed by deposition in river sediments and/or further transfer into agricultural soils. The lithology of bedrock exerts a huge effect on physicochemical properties (e.g., buffering capacities, metal species, mineral phases, etc.) of the river system, thereby potentially impacting the Cd mobility in watersheds. However, to date, little is known about the microscopic processes (e.g., dissolution, adsorption, and precipitation) controlling the migration of Cd from mines to varied watersheds. This study, therefore, aims to determine the controlling factors on Cd mobilization in two mining-impacted watersheds with contrasting bedrock lithology using both Cd and Pb isotopes. The Pb isotope ratios of sediments and soils in both watersheds fall into a binary mixing model with two isotopically distinct sources, i.e., mining wastes and bedrock. These results indicate that mining activities are the main sources of Cd in sediments and soils. However, the Cd isotope ratios reveal different Cd migration processes between the two watersheds. In the siliceous watershed, the $\delta^{114/110}$Cd values of sediments decrease from -0.116‰ in the upper reach to -0.712‰ in the lower reach, with a concomitant increase in Cd concentration, which may result from Cd adsorption by goethite due to the increased pH. In contrast, in the calcareous watershed, the Cd isotope compositions of sediments (-0.345 to -0.276‰) and the pH of river water are nearly invariable, suggesting that the adsorption and release of Cd in sediments are limited. This may result from the strong pH buffering effect due to the presence of carbonate rocks. This study highlights the different fates of Cd in siliceous and calcareous watersheds and suggests that the development of Cd pollution control policies must consider regional lithology.

1. Introduction

Cadmium (Cd) is a toxic metal that severely threatens water quality and food security (e.g., Qu et al., 2017). Mining activity may also generate a large amount of Cd-rich wastes, including acid mine drainages (AMD), tailings, slags, and dusts (e.g., Wen et al., 2015). It has been estimated that mining activities contribute approximately 0.01 to 3.9 tons of Cd to global surface runoff each year (Nriagu and Pacyna, 1988). These mining wastes may be transported into rivers followed by deposition in sediments, which serve as both sinks and sources for Cd in water bodies, thereby posing potential risks to water and soil securities (e.g., Liao et al., 2017). Consequently, deciphering the mobilization of Cd from mines to ambient watersheds is of significance to restrain the sources and processes of Cd pollution.

Conventional approaches to explore the migration and transformation of heavy metals in watersheds usually rely on bulk concentrations and chemical fractions (e.g., Qin et al., 2021; Wu et al., 2020). However, this traditional approach often has difficulty in accurately deciphering geochemical processes, particularly at the interface between solid and liquid phases. The total concentration of a metal can

* Corresponding authors.
E-mail addresses: gaoting@mail.gyig.ac.cn (T. Gao), liuchengshuai@vip.gyig.ac.cn (C. Liu).

https://doi.org/10.1016/j.watres.2022.118619
Received 23 February 2022; Received in revised form 2 May 2022; Accepted 13 May 2022
Available online 16 May 2022

often be affected not only by migration processes but also by the dilution effect (e.g., Qin et al., 2021). Selective sequential extraction is inefficient for some specific and selective species of heavy metals, such as those associated with well-crystallized Fe-oxyhydroxides (e.g., Yin et al., 2016).

With the rapid development of analytic techniques, metal stable isotopes have been shown to serve as powerful tools to trace the sources and biogeochemical processes of heavy metals in environments (e.g., Wiederhold, 2015). This is primarily because, compared with conventional approaches, metal stable isotope ratios are hard to change during dilution processes and can exactly reveal the sources and/or biogeochemical processes of metals. Previous studies have indicated that geochemical processes, including dissolution, adsorption, precipitation, and biological processes can produce pronounced Cd isotope fractionations (e.g., Horner et al., 2011; Wasylenki et al., 2014; Yan et al., 2021; Yang et al., 2021). The Cd isotope signature (e.g., $\delta^{114/110}$Cd), therefore, can be used as a tracer of Cd. During the leaching of Pb-Zn ore rocks in the lab, Zhang et al. (2016) showed that leachates are enriched in isotopically heavy Cd compared with ores, with Cd isotope fractionation ($\Delta^{114/110}Cd_{ore\text{-}leachate}$) ranging from -0.4 to -0.5‰. In addition, laboratory studies indicate that light Cd isotopes are preferentially adsorbed onto Fe/Mn oxyhydroxides (Wasylenki et al., 2014; Yan et al., 2021) and humic acid (Ratie et al., 2021) and coprecipitated into sulfide (Guinoiseau et al., 2018) and calcite (Horner et al., 2011; Xie et al., 2021). Thus, the aqueous phases are, in most cases, enriched in heavier Cd isotopes than solid phases. This has been ascribed to the shorter Cd–O bond lengths for aqueous Cd species than for most secondary minerals (Gao et al., 2021). In contrast, a recent study showed that heavy Cd isotopes are preferentially incorporated into goethite by substituting lattice Fe, owing mostly to the enrichment of heavy Cd isotopes in Cd-hydroxides (Yan et al., 2021). Moreover, a few studies have also investigated the behavior of Cd in watersheds (e.g., Yang et al., 2019; Wen et al., 2015). For example, Yang et al. (2019) observed that rivers draining sulfide mining areas have higher $\delta^{114/110}$Cd values than mine tailings and ore minerals and explained this by the rapid dissolution of ore tailings. However, it is expected that some differences in Cd isotope fractionation may exist in watersheds due to diverse microscopic geochemical processes that can mobilize Cd.

The lithology of bedrock can also be an important factor impacting the mobilization of Cd in both river and soil systems. In particular, rivers draining siliceous and calcareous rocks are often characterized by different physicochemical properties (e.g., Qin et al., 2021; Yang et al., 2019). For example, it has been suggested that in carbonate-dominated regions, the coexistence of dissolved CO_2 with carbonate minerals can result in high and stable pH in river waters (e.g., Sherlock et al., 1995). This alkaline environment is conducive to the adsorption of Cd onto secondary minerals or precipitation of Cd-rich carbonates in sediments (e.g., Wu et al., 2020), which thus restricts the migration of Cd in rivers. In contrast, this restriction usually does not work in regions dominantly covered with siliceous rocks due to their limited buffering capacity (Sherlock et al., 1995). However, few studies have focused on how geochemical processes, including dissolution, adsorption, and precipitation, may affect the mobility and isotope fractionation of Cd from mines to varied watersheds.

In this study, we collected and studied samples from two watersheds affected by mining activities. One of them was developed in a basin with siliceous bedrock (Dabaoshan), and the other was developed in a basin with calcareous bedrock (Niujiaotang) in South China. River water, sediment, soil, and mining waste (including AMD, AMD-precipitate, tailings, and mining dust) were systematically sampled for Cd isotope analyses. Given that Pb isotopes are not fractionated during biogeochemical processes (e.g., Cheng and Hu, 2010), the Pb isotope ratios were also measured here for source tracing. Our work aims to identify the source of Cd in rivers and soil and to investigate and compare factors controlling the behavior of Cd from mines to ambient watersheds. Our findings contribute to a deeper understanding of Cd behavior in mining-affected watersheds with different lithologies and eventually to improved strategies for Cd pollution control.

2. Materials and methods

2.1. Site description and sample collection

Dabaoshan (DBS) is located in Guangdong Province, southern China (113°43′13″E, 24°31′36″N) and is characterized by subtropical latosol and influenced by a subtropical monsoon climate. The bedrock under the soil is mostly sandstone, which is mainly composed of quartz (84 wt.%), muscovite (4 wt.%), and phengite (12 wt.%) (Liu et al., 2020). The DBS mine is a large-scale polymetallic sulfide deposit with main ore minerals of pyrite, chalcopyrite, pyrrhotite, sphalerite, and galena (Ye et al., 2014). After being smashed by crushers, ores were separated from rocks by flotation. Due to ~60 years of mining activity, a large quantity of AMD and AMD-precipitates (including both ore rock particles and hydrogenous minerals precipitated out of AMD) are stored in the Liwu dam and then discharged into the Hengshi (HS) River (Fig. 1a). River water, sediment, and soil samples were collected from nine sampling sites, which are distributed along the ~20-km stretches of the HS River from the tailings dam (Liu et al., 2020). For comparison, a deep soil sample (~80 cm) from the lower reach of the HS River was collected as the background soil. The pH of HS River water was measured in *situ* by a portable pH meter (HQ40D, Hach, USA). Representative samples of sulfide ores, AMD, AMD-precipitates, bedrock, and fertilizers were also collected. Details for sample collection and treatment prior to chemical analyses have been described in Liu et al. (2020).

Niujiaotang (NJT) is a small town in Guizhou Province, southern China (107°39′20″E, 26°13′54″N) and is influenced by the subtropical monsoonal climate. The area is characterized by a typical karst landform, with dolostone as the dominant bedrock (Xia et al., 2020). The NJT mine is a Pb-Zn sulfide deposit with main ore minerals of sphalerite and galena (Zhang et al., 2018). Ores were also separated from rocks through flotation. A large amount of dust was generated during ore smashing and the flotation effluent was directly discharged into the Fanjia (FJ) River. Details for sampling and treatment prior to chemical analyses were elaborated in Xia et al. (2020). Because the mining duration in this region (~20 years) is shorter than that in the DBS mine, the mining-affected scale is relatively small, and sampling was conducted within ~3 km along the FJ River from the mining area. Briefly, river water, sediment, and soil samples were collected from six sampling sites along the FJ River (Fig. 1b). Two background soils were collected from the deep layer (~80 cm) in the lower reach of the FJ River. Sulfide ore, tailings, mining dust, bedrock, and fertilizer were collected for comparison. Measurements of river pH were carried out in the field by a portable pH meter (HQ40D, Hach, USA).

2.2. Analysis of Cd and Pb concentrations

Measurements of Cd and Pb concentrations for all samples were taken by inductively coupled plasma–mass spectrometry (ICP–MS, NexION 300X, PerkinElmer, USA). Prior to measurements, ~100 mL of each liquid sample was dried on a hot plate, and ~100 mg of each solid sample was digested after being treated with HF–HNO_3 (1:3, v/v) and aqua regia. After each digested sample reached complete dryness on a hot plate at 90°C for 12 hours, it was redissolved in ~2% HNO_3 to measure the Cd and Pb concentrations. The instrument drift was calibrated by the internal standard Rh (10 μg L^{-1}). GSS-1 (Chinese National Standard soil reference sample) and BHVO-2 (United States Geological Survey reference material) were used for data quality control. Repeated measurements (n = 5) of each sample obtained the relative standard deviation (RSD) within 10%.

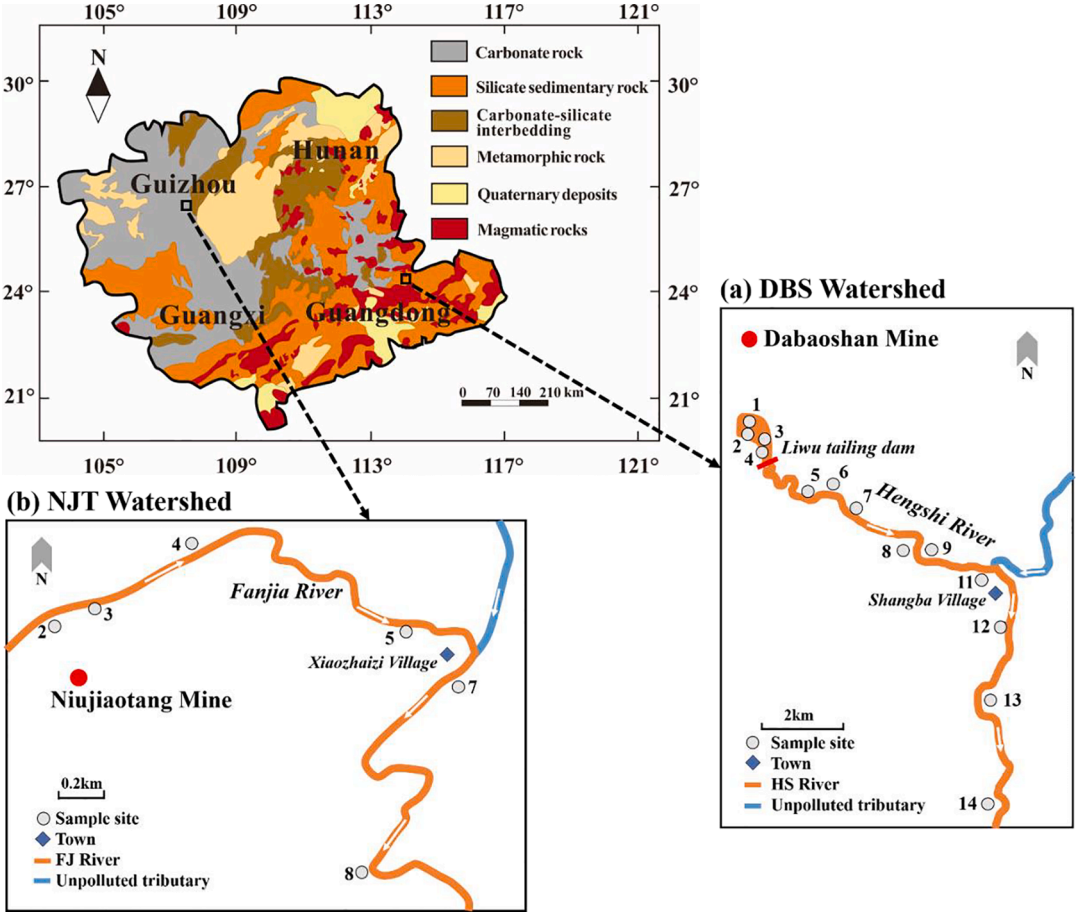

Fig. 1. Map of the study area and sampling sites in DBS (a) and NJT (b) watersheds.

2.3. Selective sequential extraction experiment

The selective sequential extraction of Cd following Tessier et al. (1979) was conducted to investigate Cd association in sediments and soils from NJT. Given the large amount of Fe (hydro)oxides present in sediments and soils from DBS, a modified Tessier method was employed to effectively extract Cd bound to well-crystallized Fe (hydro)oxides (Yin et al., 2016). The steps of the procedure are presented in Tables S1 and S2. The Cd concentrations of all extracted solutions were measured using ICP–MS (NexION 300X, PerkinElmer, USA) as mentioned above.

2.4. Mineral quantification

The mineral modes of sediments, soils, ores, and bedrock were characterized by an X-ray diffractometer (XRD, Bruker D2, Germany). Co/Kα radiation was used to generate X-rays, which were scanned over 5–85° at a speed of ~1.2°/min with a step size of ~0.02°. TOPAS V5 software (Bruker AXS, Germany) was used to quantify the mineral compositions by using the Rietveld method (e.g., Young, 1993). The uncertainty for major minerals is considered to be approximately 1–2%.

2.5. Analysis of Cd and Pb isotope ratios

All sample digestion and purification procedures were performed in a class-100 laminar flow hood, which was placed in a class-1000 clean room. All acid reagents (including HF, HCl, and HNO_3) were distilled on acid purification systems (DST-1000, Savillex, USA). Ultra-pure Milli-Q water (18.2 MΩ cm) was used during Cd purification. Approximately 100 mL of liquid samples was evaporated in perfluoroalkane (PFA) beakers (Savillex, USA) at 130°C for 30 h, and ~100 mg of solid samples and reference materials were weighed and loaded into PFA beakers (Savillex, USA). Both evaporated water samples and solid samples were treated with an ~4 mL mixture of HF-HNO_3(1:3, v/v), followed by heating at ~140°C for ~48 h. Subsequently, ~3.2 mL of aqua regia was added into dried samples and heated at ~120°C for ~48 h before beaker caps were removed and samples were dried to dryness.

The purification of Cd was conducted at the Isotope Geochemistry Laboratory of China University of Geosciences, Beijing, China. The detailed procedures for column chemistry have been reported in Tan et al. (2020). Briefly, ^{111}Cd-^{113}Cd double spikes were added to samples containing ~60 ng of Cd after dried samples were redissolved in concentrated HNO_3. The beakers were placed on a hot plate at ~100°C overnight to ensure that the sample and spike were mixed homogeneously and then evaporated to dryness. Then, the dried samples were subsequently dissolved in 2 M HCl and purified by passing through anion columns filled with AG-MP-1M resin (100-200 mesh, Bio-rad, USA). The same column procedure was repeated twice to obtain a pure Cd solution, which was then dissolved in 2% HNO_3–0.1% HF for isotopic determination.

Cd isotope ratios were determined by multiple-collector ICP–MS (MC–ICP–MS, Neptune plus, Thermo Fisher, USA) at China University of Geoscience, Beijing, China. Samples were introduced into the plasma through an Aridus-II desolvator (Teledyne CETAC Technologies Omaha, USA). Samples were measured at ~10 ppb and bracketed by a spiked NIST-3108 solution to correct for instrumental drift (Tan et al., 2020). The Cd isotope composition is expressed as $\delta^{114}/^{110}Cd$ relative to NIST-3108 and defined as:

$$\delta^{114/110}Cd(‰) = \left[\frac{(^{114}Cd/^{110}Cd)_{sample}}{(^{114}Cd/^{110}Cd)_{NIST3108}} - 1\right] \times 1000 \quad (1)$$

The analysis for each sample was repeated three times and the uncertainties were two times standard deviation (2SD) based on repeated measurements. The NIST reference material 2711a and Chinese geochemical standard reference GSS-1 were processed together with samples and yielded average $\delta^{114/110}$Cd values of 0.567 ± 0.051‰ (2SD) and 0.024 ± 0.077‰ (2SD), respectively, which are consistent with previously reported results (Li et al., 2018; Tan et al., 2020).

Lead was purified using AG1-X8 resin (200–400 mesh, Bio–Rad, USA) at the Guangdong Institute of Eco-environmental Science & Technology, China. Digested samples with ~1 μg Pb were evaporated to dryness and dissolved in a mixture of 2 M HCl and 1 M HBr (2:1, v/v). The high purity glass columns packed with ~1.2 mL resins were alternately cleaned with 6 M HCl and ultrapure water three times and then conditioned with a mixture of 2 M HCl-1 M HBr (2:1, v/v). Matrix components were eluted after ~1.5 mL of 1 M HBr and ~1.5 mL of 2 M HCl. Finally, Pb was eluted with ~1.5 mL of 6 M HCl. The total procedural blanks of Pb during this study were less than ~0.15 ng. The lead isotope ratios were measured by MC–ICP–MS (Neptune Plus, Thermo Fisher, USA) at the Institute of Geochemistry, Chinese Academy of Sciences, China. The Tl standard (NIST 997) was added to the purified sample with a Pb/Tl ratio of ~5 to correct for instrumental mass bias. The repeated measurements of reference material NIST 981 yielded an average ^{207}Pb/^{206}Pb ratio of 0.91464 ± 0.00004 (2SD, N = 45) and an average ^{208}Pb/^{206}Pb ratio of 2.16650 ± 0.00008 (2SD, N = 45), which agree with previously published data (e.g., Jeong et al., 2021).

4. Results

4.1. Mineral compositions

The mineral compositions of sediments, soils, and AMD-precipitates are presented in Table S3 and Table S4. In DBS, the sediment, soil, and AMD-precipitates are mainly composed of quartz (16.0 to 66.4 wt.%), muscovite (2.6 to 30.9 wt.%), phengite (2.5 to 24.8 wt.%), goethite (2.2 to 20.6 wt.%), kaolinite (1.9 to 15.6 wt.%), and microcline (0 to 16.8 wt.%). Trace amounts of goethite, jarosite, and hematite are found in AMD-precipitates. Sediments and soils in the NJT mainly contain quartz (1.6 to 71.2 wt.%), dolomite (0 to 98.4 wt.%), kaolinite (0 to 14.8 wt.%), and illite (0 to 16.0 wt.%). The mine tailings consist of dolomite (~97.2 wt.%) and sphalerite (~2.8 wt.%).

4.2. Cd and Pb concentrations and isotope compositions of samples from DBS

The Cd concentration of river water ranges from 0.007 to 0.035 mg L^{-1}, which is dramatically lower than that of AMD (1.35 to 1.47 mg L^{-1}). The sediment has a Cd concentration ranging from 1.79 to 17.5 mg kg^{-1}, which is higher than that of bedrock (~0.11 mg kg^{-1}). The Cd concentration of sulfide ore is ~3.76 mg kg^{-1}, which is higher than that of AMD-precipitates (1.12 to 3.56 mg kg^{-1}). Compared with the sediment, the topsoil has a relatively lower Cd concentration, varying from 0.24 to 2.59 mg kg^{-1} (Table S5).

The $\delta^{114/110}$Cd value of the AMD-precipitate varies from -0.186 to -0.030‰, which is lower than those of AMD (0.077 to 0.131‰) and sulfide ore (0.211 ± 0.042‰). The river water has a $\delta^{114/110}$Cd value ranging from 0.175 to 0.309 ‰, which is higher than that of the sediment (-0.712 to -0.116 ‰) and topsoil (-0.366 to -0.167 ‰). The $\delta^{114/110}$Cd value of the sediment from the upper reach (DC-5, 6, and 8) ranges from -0.116 to -0.183‰, which is higher than that from the lower reach (DC-11 and 13; -0.682 to -0.712‰) but closer to the $\delta^{114/110}$Cd value of the AMD-precipitate (-0.186 to -0.030‰) (Fig. 2a). Similarly, the topsoil in the upper reach has a higher $\delta^{114/110}$Cd value (DS-6, 8, 9, and 11; -0.251 to -0.167‰) than that in the lower reach (DS-12 and 14; -0.366 to -0.252‰; Fig. 2a).

The Pb concentrations of river sediments and topsoils range from 85.3 to 2602 mg kg^{-1} and from 50.5 to 1023 mg kg^{-1} respectively, which are generally higher than those of bedrock (~50.9 mg kg^{-1}). The AMD-precipitate has Pb concentrations ranging from 1936 to 3394 mg kg^{-1} and the sulfide ore has Pb concentrations of ~2666 mg kg^{-1} (Table S5). The ^{206}Pb/^{207}Pb ratios of the sediment and topsoil range between 1.1863 and 1.1900 and between 1.1863 and 1.1899, respectively, which are slightly higher than those of the sulfide ore (~1.1860) and AMD-precipitate (1.1861 to 1.1863). A higher ^{206}Pb/^{207}Pb ratio is found in the bedrock sample (~1.2523; Table S5).

4.3. Cd and Pb concentrations and isotope compositions of samples from NJT

The Cd concentrations of the sulfide ore, mine tailings, and mining dust from NJT are ~1025 mg kg^{-1}, ~316 mg kg^{-1}, and ~387 mg kg^{-1}, respectively. The river water has a low Cd concentration even below the detection limit (0.06 μg L^{-1} for our instrument). The Cd concentration of the sediment varies from 4.14 to 100 mg kg^{-1}, which is slightly higher than that of the topsoil (between 4.31 and 58.4 mg kg^{-1}). In addition, the background soil has a Cd concentration of 3.58 to 4.19 mg kg^{-1}. In

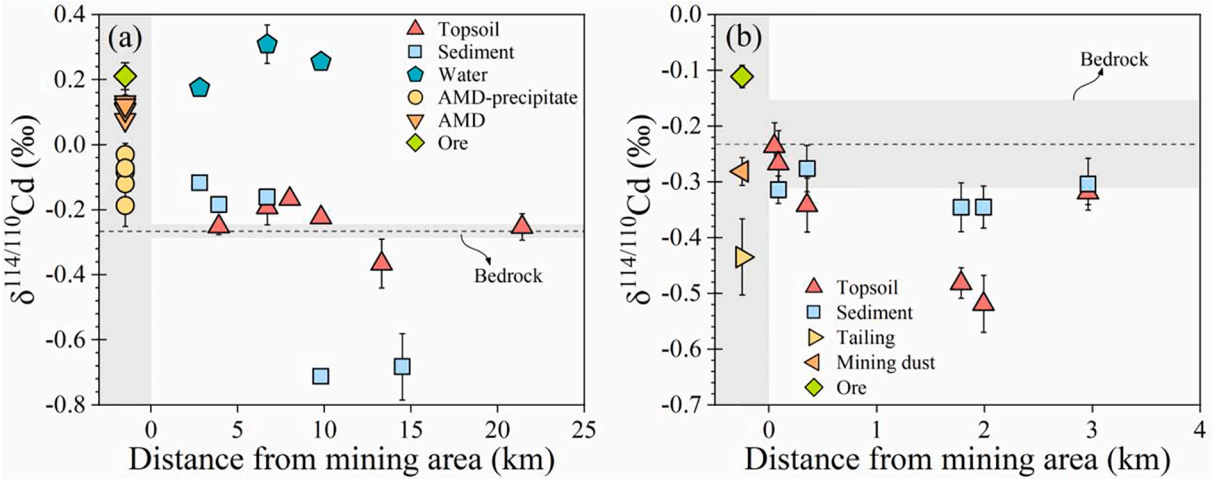

Fig. 2. Cd isotope compositions of river water, sediment, topsoil, ore, and mining waste (AMD, AMD-precipitate, tailing, and mining dust) vs. the distance from mining core in DBS (a) and NJT (b) watersheds.

particular, the Cd concentration of the calcareous bedrock (~52.9 mg kg^{-1}) is much higher than that of the siliceous bedrock from the DBS (~0.11 mg kg^{-1}) (Table S6).

The $\delta^{114/110}$Cd values of the mine tailings, sulfide ore, and mining dust are -0.435 ± 0.068‰, -0.111 ± 0.022‰, and -0.281 ± 0.025‰, respectively (Table S6). The sediment has a small range of $\delta^{114/110}$Cd values between -0.345 and -0.276‰, which generally fall between those of mine tailing and mining dust (Fig. 2b). The $\delta^{114/110}$Cd value of the topsoil ranges from -0.519 to -0.267‰ and is slightly lower than that of the sediment (Fig. 2b). The background soil has a low $\delta^{114/110}$Cd value ranging from -0.524 to -0.521‰. In addition, the calcareous bedrock has a $\delta^{114/110}$Cd value of -0.235 ± 0.081‰, which is higher than that of the topsoil.

The sediment and topsoil have Pb concentrations ranging from 85.2 to 309 mg kg^{-1} and from 91.2 to 660 mg kg^{-1}, respectively, which is higher than that of bedrock (~39.7 mg kg^{-1}). The Pb concentrations of the mine tailings, sulfide ore, and mining dust are 63.8 mg kg^{-1}, 98.4 mg kg^{-1}, and 274 mg kg^{-1}, respectively (Table S6). The sediment and topsoil along the FJ River have $^{206}Pb/^{207}Pb$ ratios ranging from 1.1596 to 1.1685 and from 1.1598 to 1.1767, respectively, which generally lie between the $^{206}Pb/^{207}Pb$ ratios of the sulfide ore (~1.1581) and background soil (1.1844 to 1.1870). The bedrock has a high $^{206}Pb/^{207}Pb$ ratio of ~1.2117 (Table S6).

4.4. Cd speciation in the sediment and soil

The results of our selective leaching experiments show that Cd in the sediment and topsoil from DBS is largely concentrated in the exchangeable fraction (33–73% for the sediment and 23–55% for the topsoil; Fig. S2a, S2b), while Cd in the sediment and topsoil from NJT is generally associated with carbonates (57–77% for sediments and 19–63% for topsoils; Fig. S2c, S2d).

5. Discussion

5.1. Pb isotope tracing

Because radiogenic Pb isotopes are not fractionated during biogeochemical processes (e.g., Cheng and Hu, 2010), Pb isotope ratios can provide accurate information about pollution sources. The Pb isotope ratios of most sediments and topsoils from the DBS watershed fall on a binary mixing line with two isotopically distinct endmembers, i.e., ore rocks and background soil (Fig. 3b). Some samples of AMD-precipitates, sediments, and topsoils are close to ore samples, indicating that they are strongly influenced by Pb pollution from the ore. Compared with the bulk silicate bedrock in this area ($^{208}Pb/^{206}Pb$ = 2.0768, $^{206}Pb/^{207}Pb$ =1.2523), even the background soil ($^{208}Pb/^{206}Pb$ = 2.0843, $^{206}Pb/^{207}Pb$ = 1.1928) might have been polluted by ore rocks. However, AMD, some sediments, topsoils and bulk silicate bedrock are not on the mixing line (Fig. 3a). These deviations from the mixing line, which are larger than the analytical uncertainty (2SD = 0.00008 for $^{208}Pb/^{206}Pb$ and 0.00004 for $^{206}Pb/^{207}Pb$), suggest the presence of other Pb sources. Indeed, sediments, bedrocks, and topsoils at DBS consist of serval minerals that have different affinities to Th and U (e.g., Riffel et al., 2016; Basak and Martin, 2013), and some differences in mineral mode exist among these samples (Table S3). Thus, the deviations can be understood

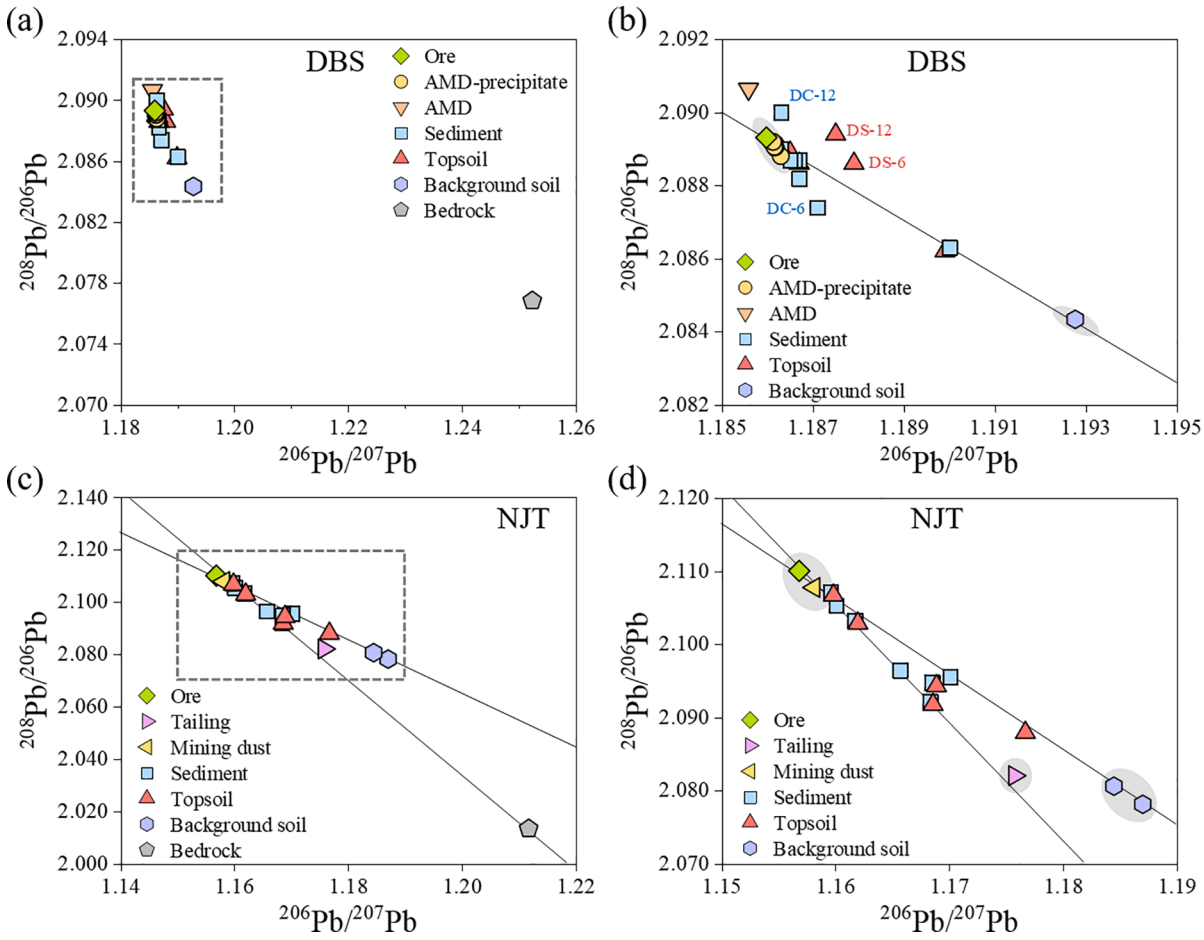

Fig. 3. Correlation of $^{206}Pb/^{207}Pb$ and $^{208}Pb/^{206}Pb$ ratio of samples from DBS (a) and NJT (c) watersheds. (b) and (d) is the enlarger of the dotted-line-defined area in (a) and (c), respectively.

if the silicate bedrock is non-homogeneous, and leaching the portion of silicates having higher $^{208}Pb/^{206}Pb$ and low $^{206}Pb/^{207}Pb$ values would make the Pb isotope ratio of the residual soil sitting below the mixing line. Correspondingly, AMD that leaches through silicates in addition to ore rocks would have a higher $^{208}Pb/^{206}Pb$ ratio than ore rocks and sit above the mixing line. Moreover, sediment samples DC-6 and DC-12 fall above and below the mixing line, respectively (Fig. 3b), which is also consistent with the non-homogeneity of sediments (Table S3). Topsoil samples DS-6 and DS-12 fall above the mixing line, which may be affected by the input of AMD (Chen et al., 2018; Qu et al., 2017) or heterogeneous mineral composition in soils (Kong et al., 2018; Wen et al., 2020) (Fig. 3b). AMD-precipitates and ore rocks are on the mixing line and have similar Pb isotope ratios, indicating that the majority of Pb in the AMD-precipitates is not from AMD, but from residual ore. Our measured Pb isotope ratio of the fertilizer has extreme values ($^{208}Pb/^{206}Pb$ = 1.9612 and $^{206}Pb/^{207}Pb$ = 1.2472) and lies below the mixing line; thus, its effect is much smaller than the pollution from ore rocks.

For some sediments and topsoils from the NJT, their Pb isotope ratios sit on the mixing line of sulfide ore rock and background soil (Fig. 3c).

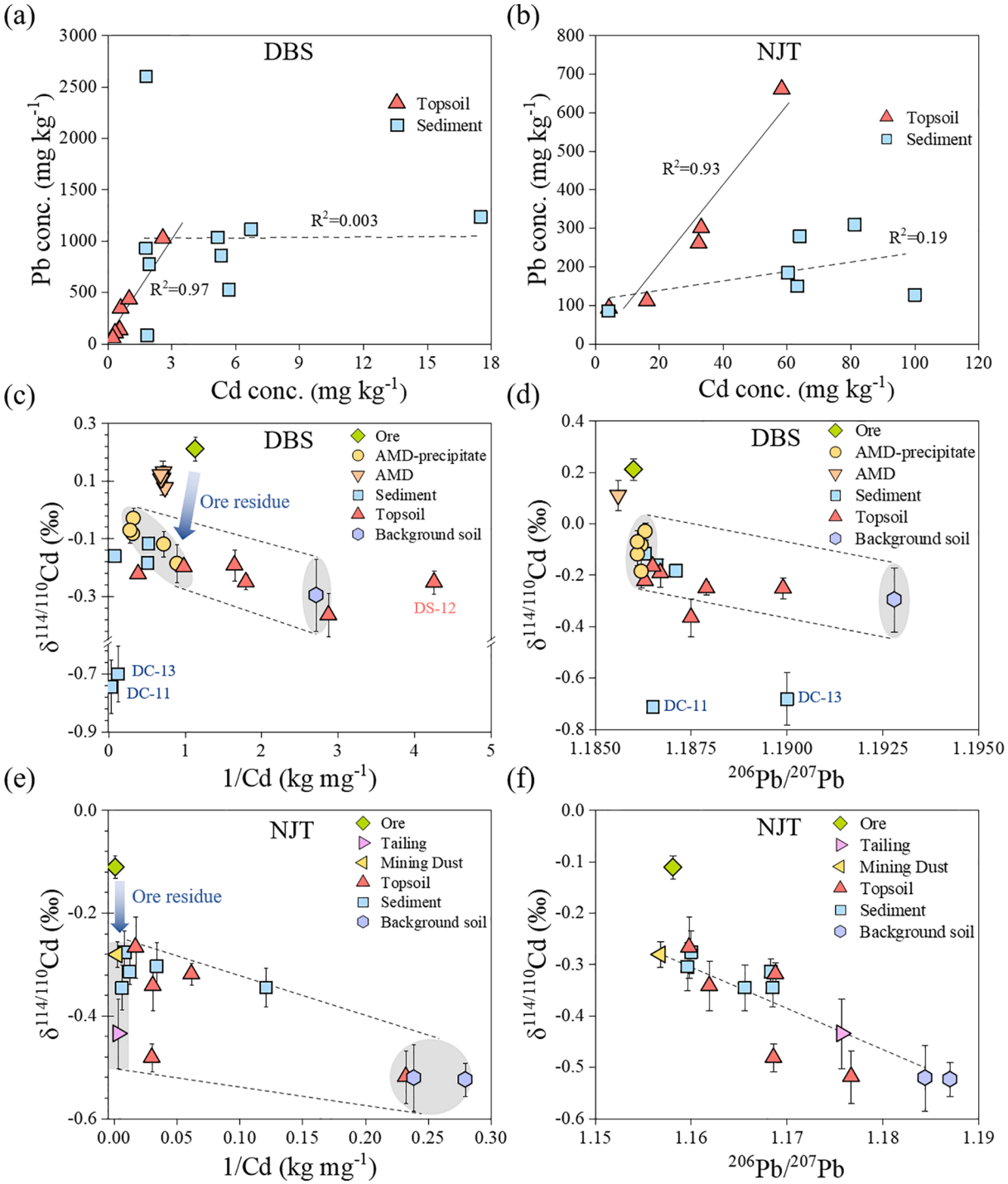

Fig. 4. Relationship of Cd and Pb concentrations in topsoils and sediments from DBS (a) and NJT (b). The solid line represents the linear fitting line of topsoils. The dashed line represents the linear fitting line of sediments. Relationship of 1/Cd and $\delta^{114/110}Cd$ of samples from DBS (c) and NJT (e) watersheds. Relationship of $^{206}Pb/^{207}Pb$ and $\delta^{114/110}Cd$ of topsoils and sediments from DBS (d) and NJT (f).

Mining dust and sulfide ore rocks have similar Pb isotope signatures, but mining dust may pollute ambient environments more easily. However, some topsoils, river sediments, mine tailings, and bedrock have Pb isotopes lying below the mixing line (Fig. 3c). This occurs because the bedrock is largely composed of carbonates which contain more U than Th and contribute to lower $^{208}Pb/^{206}Pb$ ratios than silicate rocks (Basak and Martin, 2013; Wen et al., 2020). The background soil contains a tiny fraction of carbonate. However, some topsoils and river sediments contain significant amounts of dolomite, and the mine tailings are a mixture of dolomite and sphalerite (Table S4). Thus, the Pb isotope ratios of all studied samples can be explained by the mixing of sulfide ore rocks, the silicate fraction of ambient rocks (i.e., background soil) and the carbonate fraction of the ambient rock (i.e., bedrock). The mine tailing can be considered as a mixture of bedrock and mining dust (Fig. 3d). Again, the extreme Pb isotope ratio of the fertilizer suggests its limited contribution (Fig. 3b).

5.2. Sources of Cd in sediment and soil

Since both Cd and Pb are chalcophile elements with similar geochemical properties, Cd is usually accompanied by Pb in sulfide-polluted media (e.g., Huang et al., 2020; He et al., 2019). Indeed, in the present study, the concentrations of Cd and Pb in topsoils show a significant positive correlation in both watersheds (Fig. 4a, b), suggesting similar sources of Cd and Pb in topsoils. However, Cd and Pb concentrations in sediments are decoupled (Fig. 4a, b), especially in DBS, implying that Cd and Pb behave differently in these samples. Cd isotopes can be used to investigate the origin of the difference. Given the evident difference in the Cd isotope composition among the sulfide ore rock, mining waste, and background soil (Fig. 4c, d), the Cd isotope compositions of the sediment and soil samples may also reflect mixing processes of various sources.

For most topsoil and some sediment samples from DBS, binary mixing relationships can be found in both $\delta^{114/110}Cd$–1/Cd (i.e., inverse concentration) and $\delta^{114/110}Cd$–$^{206}Pb/^{207}Pb$ diagrams, where AMD-precipitates and background soil are defined as the two end-members (Fig. 4c, d). This is consistent with the conclusion drawn based on Pb isotopes (discussed in section 5.1). Moreover, sediment samples close to the mining area, including DC-5, DC-6, and DC-8, have Cd isotope compositions (-0.183 to -0.116‰) similar to that of the AMD-precipitate (-0.186 to -0.030‰), suggesting that AMD-precipitates are also the main Cd source to river sediments. However, this mixing relationship cannot be used to explain the differences in $\delta^{114/110}Cd$ values among the sulfide ore rock, AMD and AMD-precipitates, and $\delta^{114/110}Cd$ values of some sediments located in the lower reach (e.g., DC-11 and DC-13), which may be related to the post-depositional processes in the river system (discussed in section 5.3 and section 5.4).

In comparison, the Cd and Pb isotope ratios appear to show slightly different mixing endmembers for sediments and topsoils from NJT (Fig. 4e, f). In the $\delta^{114/110}Cd$–1/Cd plot (Fig. 4e) and $\delta^{114/110}Cd$–$^{206}Pb/^{207}Pb$ diagram (Fig. 4f), sediments and topsoils can be circumscribed by three end-members: mining dust, mine tailing and background soil. This agrees with the tracing result from the $^{206}Pb/^{207}Pb$ -$^{208}Pb/^{206}Pb$ diagram (Fig. 3c, d). However, sulfide has a distinctly different $\delta^{114/110}Cd$ value from that of mine tailings or mining dust, which could originate from Cd isotope fractionation during leaching processes (discussed in section 5.3). Moreover, the difference (~0.320‰) between the $\delta^{114/110}Cd$ value of sulfide ore from DBS and that from NJT is likely caused by the difference in mineral composition if carbonate and sulfide minerals are characterized by different Cd isotope signals; the sulfide ores in NJT contain a large amount of carbonate (~85.2 wt.%), while those in DBS mainly consist of sulfide minerals (e.g., pyrite).

5.3. Cd isotope fractionation in mining wastes

Previous studies have shown that Cd isotopes can be highly fractionated due to leaching (Zhang et al., 2016), adsorption onto minerals (Yan et al., 2021; Wasylenki et al., 2014), and coprecipitation into minerals (Yan et al., 2021). Although this fractionation could complicate the source determination using only Cd isotopes, it can help to elucidate geochemical processes that Pb isotopes are not able to detect.

In DBS, the AMD-precipitate and sulfide ore have similar Pb isotope ratios, but the $\delta^{114/110}Cd$ value of the AMD-precipitate is significantly lower than that of the sulfide ore ($\Delta^{114/110}Cd_{ore–AMD\text{-}precipitate} = 0.241$ to 0.397‰). Similarly, the $\delta^{114/110}Cd$ value of the mining dust from the NJT is significantly lower than that of the sulfide ore ($\Delta^{114/110}Cd_{ore–mining\ dust} = 0.170$‰), although mining dust and sulfide ore have similar Pb isotope ratios. Because the original sulfide ore rocks were washed first after being mined, these discrepancies between the $\delta^{114/110}Cd$ values of AMD-precipitate/mining dust and ores can be explained by the leaching of Cd. The leaching experiment conducted by Zhang et al. (2016) showed that isotopically heavy Cd is preferentially released into liquid phases. Additionally, the Cd concentration of AMD-precipitate and mining dust is much lower than that of sulfide ore (Table S5, S6). These results suggest that ore washing may lead to a significant removal of Cd in ores and, therefore, the enrichment of light Cd isotopes in ore residues.

The $\delta^{114/110}Cd$ values of AMD (0.077 to 0.131‰) in DBS are lower than those of sulfide ores (0.211 ± 0.042‰). This observation contrasts with the result of the leaching experiment that heavy Cd is preferentially released into the aqueous solution (Zhang et al., 2016). This observation is also inconsistent with the Cd adsorption on Fe (oxyhydr)oxides. Based on XRD, the AMD-precipitate contains a significant amount of Fe (oxyhydr)oxides (e.g., goethite) (Table S3). AMD is a sulfuric acid-rich solution with pH < 2.5 (Table S5). Boily et al. (2005) found that little dissolved Cd could be adsorbed by goethite at pH < 5.0, so Cd adsorption onto Fe (oxyhydr)oxides could be limited in the tailings dam. Even if adsorption occurs, lighter Cd isotopes are preferentially adsorbed onto solid phases (Yan et al., 2021), thereby elevating the $\delta^{114/110}Cd$ value of AMD rather than decreasing it. Alternatively, the dissolved Cd in the AMD may migrate into the AMD-precipitates through coprecipitation with Fe (oxyhydr)oxides, which widely exist in an AMD pool (e.g., Chen et al., 2018). It is suggested that Cd incorporation into goethite by substitution for lattice Fe prefers heavy Cd isotopes due to the release and reprecipitation of isotopically heavy Cd during the transformation of ferrihydrite to goethite (Yan et al., 2021). Therefore, isotopically heavy Cd in AMD may preferentially coprecipitate with Fe (oxyhydr) oxides, resulting in light isotope enrichment in AMD (Fig. 4c). The other plausible explanation, which is also consistent with the Pb isotope results of AMD, is that leachates from both ore rocks and silicates contribute to AMD. The Pb isotope ratios of AMD suggest that AMD receives the contribution of both ore rocks and silicates which pulled AMD slightly above the mixing line (Fig. 3b, discussed in section 5.1). Because silicate rocks have lower $\delta^{114/110}Cd$ values (e.g., $\delta^{114/110}Cd_{bedrock} = -0.265 \pm 0.008$‰), the leachate from leaching silicates would have a $\delta^{114/110}Cd$ value higher than silicates but lower than ore rocks.

Moreover, the Pb isotope ratio of the mine tailings suggests that both sulfide ore and carbonate bedrock have a significant contribution to the mine tailing in the NJT, while the $\delta^{114/110}Cd$ value of mine tailings is significantly lower than that of the ore ($\Delta^{114/110}Cd_{ore–tailing} = 0.324$‰) and bedrock ($\Delta^{114/110}Cd_{bedrock–tailing} = 0.200$‰). Leaching of sulfide ore rock, therefore, is necessary to explain the lower $\delta^{114/110}Cd_{mine\ tailing}$, similar to mine dust in NJT or AMD-precipitates in DBS. Besides, heavy Cd isotopes are preferentially leached out from limestone (Imseng et al., 2018), which may lead to the Cd isotope composition of mine tailings being lower than that of bedrock. Overall, both processes are required to explain the Cd and Pb isotope ratios of mine tailings in the NJT.

5.4. Cd isotope fractionation in the rivers

The Cd isotope compositions of sediments show distinctly different variations between the two watersheds (Fig. 2). In DBS, the river sediments (-0.183 to -0.116‰) and water (0.175 ± 0.010‰) from the first ~10 km of the HS River have Cd isotope compositions similar to those of AMD-precipitates (average $\delta^{114/110}$Cd of -0.098 ± 0.105‰, 2SD) and AMD (average $\delta^{114/110}$Cd of 0.109 ± 0.037‰, 2SD), respectively (Fig. 2a). These results appear to suggest that the mining waste after being discharged from the tailings dam is transported along the HS River followed by deposition in sediments. It is worth noting that the Cd concentration of sediments gradually increases during the first ~10 km of the HS River (Fig. S1). The slope rate of the riverbed declines in this stretch of the HS River, which leads to the high level of settling of mining waste particles (Chen et al., 2018). After ~10 km from the mining site, the Cd isotope compositions of sediments in the HS River decrease (Fig. 2a), while the Pb isotope ratios of sediments vary only slightly (Table S5). These observations indicate that the adsorption and/or coprecipitation of Cd onto/into sediments (most likely goethite based on XRD, Table S3) may occur during Cd transportation in rivers, which may fractionate Cd isotopes.

Yan et al. (2021) suggested that the coprecipitation of Cd into Fe (oxyhydr)oxides preferentially takes up isotopically heavy Cd, which contrasts with the decreased $\delta^{114/110}$Cd of sediments from the upper to lower reach (Fig. 2a). This implies that the possible coprecipitation of goethite has limited effects on Cd isotope fractionation. Instead, it is more likely that these changes in $\delta^{114/110}$Cd of sediments originate primarily from the enhanced adsorption of Cd onto goethite as the pH value of river water increases due to dilution and silicate buffering effects (Yang et al., 2019). A pioneering study has shown that Cd adsorption on Fe (oxyhydr)oxides prefers light Cd isotopes and that the adsorption capacity increases dramatically as the pH increases from 6.0 to 8.0 (Yan et al., 2021). As such, some Cd may be adsorbed onto Fe (oxyhydr)oxides in sediments due to the increased river pH (6.4 to 8.1) (Fig. S3a). Previous studies have shown that the adsorbed Cd is mainly transformed into the exchangeable form (Fan et al., 2007), and this Cd fraction often enriches light isotopes (Zhong et al., 2021). Therefore, the positive correlation between the river pH and the amount of exchangeable Cd in sediments proves that the increased pH causes more adsorbed Cd, which thus results in the decreased $\delta^{114/110}$Cd value of sediments along the HS River (Fig. 5a).

In contrast, the Cd isotope compositions of sediments in the NJT are nearly invariable along the FJ River (Fig. 2b), which is likely caused by the low dissolution rate of carbonates in an alkaline environment. High and stable pH values are observed in FJ River water, which may be the result of the powerful acid buffering potential of calcareous rocks (Fig. S3b, e.g., Raymond et al., 2009):

$$Ca_xMg_{1-x}(CO_3)_2 + 2H^+ = 2HCO_3^- + (1-x)Mg_x^{2+} + xCa^{2+}$$

Carbonates may neutralize acid from mine drainage and produce bicarbonate to maintain the high pH of river water, which has also been observed in other carbonate-dominated watersheds (e.g., Mayo et al., 2000; Qin et al., 2021). Alkaline conditions can inhibit the dissolution of carbonates (Pokrovsky et al., 1999), the dominant fraction of sediments from NJT according to the selective sequential extraction result (Fig. S3d). However, a high pH may enhance the adsorption and/or precipitation of dissolved Cd (e.g., Wu et al., 2020), which can produce Cd isotope fractionation (e.g., Wasylenki et al., 2014; Yan et al., 2021). The river water shows extremely low Cd concentrations, which are even below the detection limit (Table S6), suggesting that most dissolved Cd has been adsorbed or precipitated before being discharged into rivers. As a result, river water may only contribute little dissolved Cd to sediments and, consequently, may have a limited effect on the Cd isotope composition of sediment.

6. Conclusions and implications

Based on the Cd isotope compositions of river water, sediments, soils, bedrock, and mining wastes developed in siliceous (DBS) and calcareous (NJT) basins, this study unravels the mechanisms controlling Cd mobility and Cd isotope fractionation from the mine to ambient watersheds. Our results show that mining activities are the main supplier of Cd in river-soil systems around both mining areas, whereas the extent and level of Cd pollution are very different. In DBS, the decrease in $\delta^{114/110}$Cd in sediments indicates the enhanced adsorption of Cd by Fe oxides in the river due to the elevated pH. In the NJT watershed, the invariable $\delta^{114/110}$Cd values of sediments suggest that the adsorption and release of Cd in sediments are limited because of the high and stable pH caused by the carbonate buffer.

In this way, to limit Cd migration, developing different policies in siliceous and calcareous watersheds is crucial. For a siliceous watershed, it is necessary to restrain the release of adsorbed Cd in sediments by increasing the river pH through limestone or hydrated lime (Luo et al., 2020). In a calcareous watershed, the acidity produced by sulfide mineral oxidation can be partially or completely offset by carbonate rock, resulting in neutral or weakly alkaline mine water (Sherlock et al., 1995). Therefore, natural geochemical processes for acid neutralization and precipitation–adsorption of metals may be an economical way to

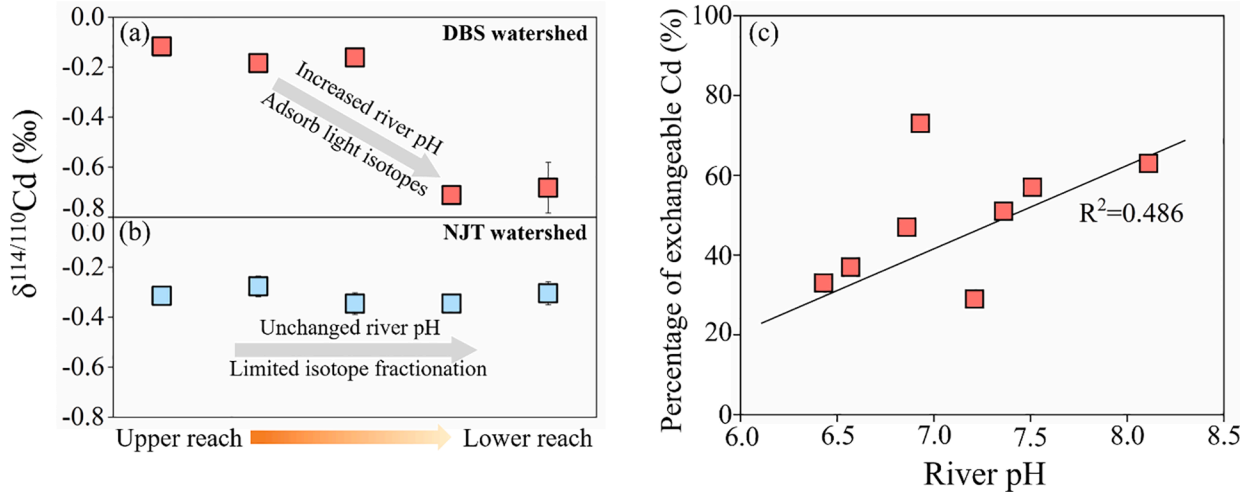

Fig. 5. The Cd isotope compositions of sediments along the HS River (a, DBS watershed) and FJ River (b, NJT watershed). The data were plotted according to the sequence of sampling sites. The correlation of river pH and the percentage of exchangeable Cd in sediments (c).

prevent AMD in a calcareous watershed. In addition, this study also shows the different Cd isotope fractionation mechanisms in the two watersheds. Therefore, the influence of lithology needs to be taken into account and interpreted with caution before using the Cd isotope tool for tracing pollution. For example, combining Pb isotopes may improve the accuracy of source tracing in a complex area.

Declaration of Competing Interest

The authors declare that they have no known competing financial interests or personal relationships that could have appeared to influence the work reported in this paper.

Acknowledgments

We thank Dr. Yang Tang, Zhuo Lu, and Hui Chang for help during sample analysis. The research was supported by the National Natural Science Foundations of China (42025705 and 41921004), the Strategic Priority Research Program (XDB40020400), the Frontier Science Research Programme (QYZDB-SSW-DQC046) of the Chinese Academy of Sciences, and GDAS' Project of Science and Technology Development (2019GDASYL-0104016)

Supplementary materials

Supplementary material associated with this article can be found, in the online version, at doi:10.1016/j.watres.2022.118619.

References

Basak, C., Martin, E.E., 2013. Antarctic weathering and carbonate compensation at the Eocene–Oligocene transition. Nat. Geosci. 6 (2), 121–124.
Boily, J.-F., Sjöberg, S., Persson, P., 2005. Structures and stabilities of Cd(II) and Cd(II)-phthalate complexes at the goethite/water interface. Geochim. Cosmochim. Acta 69 (13), 3219–3235.
Chen, M., Lu, G., Wu, J., Yang, C., Niu, X., Tao, X., Shi, Z., Yi, X., Dang, Z., 2018. Migration and fate of metallic elements in a waste mud impoundment and affected river downstream: a case study in Dabaoshan Mine, South China. Ecotoxicol. Environ. Saf. 164, 474–483.
Cheng, H., Hu, Y., 2010. Lead (Pb) isotopic fingerprinting and its applications in lead pollution studies in China: a review. Environ. Pollut. 158, 1134–1146.
Fan, Q., He, J., Xue, H., LÜ, C., Liang, Y., Saruli, Sun, Y., Shen, L, 2007. Competitive adsorption, release and speciation of heavy metals in the Yellow River sediments, China. Environ. Geol. 53 (2), 239–251.
Gao, T., Liu, Y., Xia, Y., Zhu, J.-M., Wang, Z., Qi, M., Liu, Y., Ning, Z., Wu, Q., Xu, W., Liu, C., 2021. Cadmium isotope compositions of Fe-Mn nodules and surrounding soils: implications for tracing Cd sources. Fundam. Res. 1, 269–276.
Guinoiseau, D., Galer, S.J.G., Abouchami, W., 2018. Effect of cadmium sulphide precipitation on the partitioning of Cd isotopes: Implications for the oceanic Cd cycle. Earth Planet. Sci. Lett. 498, 300–308.
He, B., Zhao, X., Li, P., Liang, J., Fan, Q., Ma, X., Zheng, G., Qiu, J., 2019. Lead isotopic fingerprinting as a tracer to identify the pollution sources of heavy metals in the southeastern zone of Baiyin, China. Sci. Total Environ. 660, 348–357.
Horner, T.J., Rickaby, R.E.M., Henderson, G.M., 2011. Isotopic fractionation of cadmium into calcite. Earth Planet. Sci. Lett. 312, 243–253.
Huang, Y., Zhang, S., Chen, Y., Wang, L., Long, Z., Hughes, S.S., Ni, S., Cheng, X., Wang, J., Li, T., Wang, R., Liu, C., 2020. Tracing Pb and possible correlated Cd contamination in soils by using lead isotopic compositions. J. Hazard. Mater. 385, 121528.
Imseng, M., Wiggenhauser, M., Keller, A., Müller, M., Rehkämper, M., Murphy, K., Kreissig, K., Frossard, E., Wilcke, W., Bigalke, M., 2018. Fate of Cd in Agricultural Soils: A Stable Isotope Approach to Anthropogenic Impact, Soil Formation, and Soil-Plant Cycling. Environ. Sci. Technol. 52 (4), 1919–1928.
Jeong, H., Ra, K., Choi, J.Y., 2021. Copper, zinc and lead isotopic delta values and isotope ratios of various geological and biological reference materials. Geostand. Geoanal. Res. 45 (3), 551–563.
Kong, J., Guo, Q., Wei, R., Strauss, H., Zhu, G., Li, S., Song, Z., Chen, T., Song, B., Zhou, T., Zheng, G., 2018. Contamination of heavy metals and isotopic tracing of Pb in surface and profile soils in a polluted farmland from a typical karst area in southern China. Sci. Total Environ. 637-638, 1035–1045.
Li, D., Li, M.-L., Liu, W.-R., Qin, Z.-Z., Liu, S.-A., 2018. Cadmium isotope ratios of standard solutions and geological reference materials measured by MC-ICP-MS. Geostand. Geoanal. Res. 42, 593–605.
Liao, J., Chen, J., Ru, X., Chen, J., Wu, H., Wei, C., 2017. Heavy metals in river surface sediments affected with multiple pollution sources, South China: Distribution, enrichment and source apportionment. J. Geochem. Explor. 176, 9–19.
Liu, Y., Gao, T., Xia, Y., Wang, Z., Liu, C., Li, S., Wu, Q., Qi, M., Lv, Y., 2020. Using Zn isotopes to trace Zn sources and migration pathways in paddy soils around mining area. Environ. Pollut. 267, 115616.
Luo, C., Routh, J., Dario, M., Sarkar, S., Wei, L., Luo, D., Liu, Y., 2020. Distribution and mobilization of heavy metals at an acid mine drainage affected region in South China, a post-remediation study. Sci. Total Environ. 724, 138122.
Mayo, A.L., Petersen, E.C., Kravits, C., 2000. Chemical evolution of coal mine drainage in a non-acid producing environment, Wasatch Plateau, Utah, USA. J. Hydrol. 236 (1), 1–16.
Nriagu, J.O., Pacyna, J.M., 1988. Quantitative assessment of worldwide contamination of air, water and soils by trace metals. Nature 333 (6169), 134–139.
Pokrovsky, O.S., Schott, J., Thomas, F., 1999. Dolomite surface speciation and reactivity in aquatic systems. Geochim. Cosmochim. Acta 63, 3133–3143.
Qin, W., Han, D., Song, X., Liu, S., 2021. Sources and migration of heavy metals in a karst water system under the threats of an abandoned Pb–Zn mine, Southwest China. Environ. Pollut. 277, 116774.
Qu, L., Xie, Y., Lu, G., Yang, C., Zhou, J., Yi, X., Dang, Z., 2017. Distribution, fractionation, and contamination assessment of heavy metals in paddy soil related to acid mine drainage. Paddy Water Environ. 15, 553–562.
Ratie, G., Chrastny, V., Guinoiseau, D., Marsac, R., Vankova, Z., Komarek, M., 2021. Cadmium isotope fractionation during complexation with humic acid. Environ. Sci. Technol. 55, 7430–7444.
Raymond, P.A., Oh, N.-H., 2009. Long term changes of chemical weathering products in rivers heavily impacted from acid mine drainage: Insights on the impact of coal mining on regional and global carbon and sulfur budgets. Earth Planet. Sci. Lett. 284 (1), 50–56.
Riffel, S.B., Vasconcelos, P.M., Carmo, I.O., Farley, K.A., 2016. Goethite (U–Th)/He geochronology and precipitation mechanisms during weathering of basalts. Chem. Geol. 446, 18–32.
Sherlock, E.J., Lawrence, R.W., Poulin, R., 1995. On the neutralization of acid rock drainage by carbonate and silicate minerals. Environ. Geol. 25 (1), 43–54.
Tan, D., Zhu, J.-M., Wang, X., Han, G., Lu, Z., Xu, W., 2020. High-sensitivity determination of Cd isotopes in low-Cd geological samples by double spike MC-ICP-MS. J. Anal. At. Spectrom. 35, 713–727.
Tessier, A., Campbell, P.G.C., Bisson, M., 1979. Sequential extraction procedure for the speciation of particulate trace-metals. Anal. Chem. 51, 844–851.
Wasylenki, L.E., Swihart, J.W., Romaniello, S.J., 2014. Cadmium isotope fractionation during adsorption to Mn oxyhydroxide at low and high ionic strength. Geochim. Cosmochim. Acta 140, 212–226.
Wen, H., Zhang, Y., Cloquet, C., Zhu, C., Fan, H., Luo, C., 2015. Tracing sources of pollution in soils from the Jinding Pb-Zn mining district in China using cadmium and lead isotopes. Appl. Geochem. 52, 147–154.
Wen, Y., Li, W., Yang, Z., Zhang, Q., Ji, J., 2020. Enrichment and source identification of Cd and other heavy metals in soils with high geochemical background in the karst region, Southwestern China. Chemosphere 245, 125620.
Wiederhold, J.G., 2015. Metal stable isotope signatures as tracers in environmental geochemistry. Environ. Sci. Technol. 49, 2606–2624.
Wu, W., Qu, S., Nel, W., Ji, J., 2020. The impact of natural weathering and mining on heavy metal accumulation in the karst areas of the Pearl River Basin, China. Sci. Total Environ. 734, 139480.
Xia, Y., Gao, T., Liu, Y., Wang, Z., Liu, C., Wu, Q., Qi, M., Lv, Y., Li, F., 2020. Zinc isotope revealing zinc's sources and transport processes in karst region. Sci. Total Environ. 724, 138191.
Xie, X., Yan, L., Li, J., Guan, L., Chi, Z, 2021. Cadmium isotope fractionation during Cd-calcite coprecipitation: Insight from batch experiment. Sci. Total Environ. 760, 143330.
Yan, X., Zhu, M., Li, W., Peacock, C.L., Ma, J., Wen, H., Liu, F., Zhou, Z., Zhu, C., Yin, H., 2021. Cadmium isotope fractionation during adsorption and substitution with iron (Oxyhydr)oxides. Environ. Sci. Technol. 55 (17), 11601–11611.
Yang, S., Feng, W., Wang, S., Chen, L., Zheng, X., Li, X., Zhou, D., 2021a. Farmland heavy metals can migrate to deep soil at a regional scale: A case study on a wastewater-irrigated area in China. Environ. Pollut. 281, 116977.
Yang, W.J., Ding, K.B., Zhang, P., Qiu, H., Cloquet, C., Wen, H.J., Morel, J.L., Qiu, R.L., Tang, Y.T., 2019. Cadmium stable isotope variation in a mountain area impacted by acid mine drainage. Sci. Total Environ. 646, 696–703.
Ye, L., Liu, T., Yang, Y., Gao, W., Pan, Z., Bao, T., 2014. Petrogenesis of bismuth minerals in the Dabaoshan Pb-Zn polymetallic massive sulfide deposit, northern Guangdong Province, China. J. Asian Earth Sci. 82, 1–9.
Yin, H., Tan, N., Liu, C., Wang, J., Liang, X., Qu, M., Feng, X., Qiu, G., Tan, W., Liu, F., 2016. The associations of heavy metals with crystalline iron oxides in the polluted soils around the mining areas in Guangdong Province, China. Chemosphere 161, 181–189.
Young, R., 1993. The rietveld method. Oxford University Press, NYC, NY, USA.
Zhang, J., Wei, H., Yang, R., Gao, J., Ou, Y., 2018. Study on distribution characteristics of heavy metals in tailing from niujiaotang lead-zinc mine area, Duyun City, Guizhou Province. Nonferr. Metal. Eng. 8, 122–127 in Chinese.
Zhang, Y., Wen, H., Zhu, C., Fan, H., Luo, C., Liu, J., Cloquet, C., 2016. Cd isotope fractionation during simulated and natural weathering. Environ. Pollut. 216, 9–17.
Zhong, S., Li, X., Li, F., Liu, T., Huang, F., Yin, H., Chen, G., Cui, J., 2021. Water management alters cadmium isotope fractionation between shoots and nodes/leaves in a soil-rice system. Environ. Sci. Technol. 55 (19), 12902–12913.